INTERNATIONAL JOURNAL OF HYDROGEN ENERGY XXX (2016) 1–11

Available online at www.sciencedirect.com

ScienceDirect

journal homepage: www.elsevier.com/locate/he

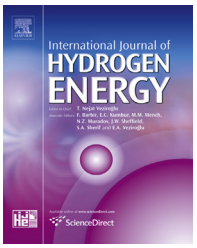

Production of hydrogen via steam reforming of acetic acid over Ni and Co supported on La_2O_3 catalyst

Walid Nabgan [a], *Tuan Amran Tuan Abdullah* [a,b,*], *Ramli Mat* [b], *Bahador Nabgan* [a], *Aishah Abdul Jalil* [a], *Lutfi Firmansyah* [a], *Sugeng Triwahyono* [c]

[a] *Centre of Hydrogen Energy, Institute of Future Energy, Universiti Teknologi Malaysia, 81310 UTM Skudai, Johor, Malaysia*

[b] *Department of Chemical Engineering, Universiti Teknologi Malaysia, 81310 UTM Skudai, Johor, Malaysia*

[c] *Centre for Sustainable Nanomaterials (CSNano), Department of Chemistry, Universiti Teknologi Malaysia, 81310 UTM Skudai, Johor, Malaysia*

ARTICLE INFO

Article history:
Received 20 September 2015
Received in revised form
26 April 2016
Accepted 26 April 2016
Available online xxx

Keywords:
Hydrogen
Acetic acid
Steam reforming
Bimetallic catalyst
Nickel–Cobalt (Ni–Co)

ABSTRACT

Nickel (Ni)-cobalt (Co) supported on lanthanum (III) oxide (La_2O_3) catalyst was prepared via impregnation technique to study the steam reformation of acetic acid for hydrogen generation by using one-step fixed bed reactor. Moreover, in order to specify the physical and the chemical attributes of the catalyst, X-ray diffraction (XRD), nitrogen physisorption, temperature-programmed reduction (TPR), temperature-programmed desorption of ammonia and carbon dioxide (TPD-NH_3 and CO_2), scanning electron microscopy (SEM), and thermogravimetric analysis (TGA) methods were employed. The nitrogen physisorption analysis showed that the presence of Co on Ni/La_2O_3 improved the textural properties of the catalyst by increasing the surface area, the pore diameter and the pore volume of the catalyst. This improved the dispersion of metal particle and caused a reduction in the size of metal particle, and consequently, increased the catalytic activity, as well as the resistance to coke formation. On top of that, the condensation and the dehydration reactions during acetic acid steam reforming created carbon deposition on acidic site of the catalyst, which resulted in the deactivation of catalyst and the formation of coke. Besides, in this study, Ni/La_2O_3 contributed to a high acetic acid conversion (100%) at 700 °C, but it produced more coking compared to Ni–Co/La_2O_3 and Co/La_2O_3 catalysts.

* *Corresponding author*. Centre of Hydrogen Energy, Institute of Future Energy, Universiti Teknologi Malaysia, 81310 UTM Skudai, Johor, Malaysia. Tel.: +60 75535549.
E-mail address: tamran@cheme.utm.my (T.A.T. Abdullah).

http://dx.doi.org/10.1016/j.ijhydene.2016.04.176
0360-3199/

Introduction

In the current time of growing ecological uncertainties and declining petroleum resources, renewable energy sources are extremely favorable [1]. With the intention of encouraging a new sustainable expansion, numerous replacements of renewable fuels are presently being utilized, such as ethanol and biodiesel [2–5]. Thus, within these past years, the attention given to the conversion of biomass to hydrogen-rich gas has raised significantly because hydrogen is considered to be a green, clean energy carrier in the future [6]. In fact, one of the numerous renewable feedstock sources and one of the major bio-oil components generation is acetic acid (17–30%) [7–10], which has been widely used and achieved by other research groups. Acetic acid can be produced from bio-oil by fermentation process [11–13]. The detail of fermentation process has been investigated by previous research [14–16].

Acetic acid has been used as a model compound of bio-oil for hydrogen production [17–21]. The thermodynamic examination on steam reforming of acetic acid has exposed that methane is the major reaction product at temperate temperatures, while high water/acetic acid molar ratio and upper temperatures regard the generation of hydrogen-rich gas [17,18]. Moreover, by using fixed-bed micro-reactor, experimental studies on steam reforming of acetic acid have been accomplished with cobalt-promoted nickel catalysts [19] and marketable Ni-based catalysts [22]. Nonetheless the catalysts' coking and formation of unwanted products, such as acetaldehyde, methane, etc., were the major problems faced throughout these experimentations. For instance, Lan et al. [23] looked into syngas and hydrogen-rich gas production from bio oil using calcined dolomite catalyst. He found that the optimum temperature for bio oil conversion to syngas was 700 °C with around 80 wt% of conversion. On the other hand, the cost of the catalyst is high due to the high amount of catalyst used to increase the steam reforming reaction rate, such as Pd catalyst, which was used for hydrogen generation from ethanol in 2001 [24], has been stated as a problem of the previous work. As indicated above, many metals can be used in steam reforming, but Ni is one of the few active metals used in conventional steam reforming catalysts due to the low price and good activity of Ni compared to the more expensive noble metals.

On top of that, a few techniques that pose disadvantages are related to hydrogen production, such as partial oxidation (POX), total oxidation (TOX), two-step reforming, and auto thermal reforming (ATR). POX, which has low natural H_2/CO ratio, is a disadvantage for applications that require a ratio of >2.0. This technique also needs very high process operating temperatures, high temperature heat recovery, and soot formation/handling that adds to process complexity. Moreover, the two-step reforming requires higher process temperature than that required for steam reforming and also requires oxygen. Meanwhile, the auto thermal reforming (ATR) technique is limited in commercial experience and requires oxygen [25]. Compared to these techniques for acetic acid conversion, steam reforming is selected since this process can be carried out at a low temperature and gives a high H_2/CO_2 production ratio [24,26].

According to previous research, the Ni-based catalysts were found to be highly active in terms of acetic acid conversion and hydrogen selectivity [27–29]. Pant et al. [11] applied Ni–Co/CeO_2/ZrO_2 catalyst and discovered that 88% of the acetic acid was converted to product at 600 °C by using unsupported Ni–Co catalyst. Meanwhile, Vagia et al. (2008) claimed that they had only reached 53% of conversion of acetic acid at a temperature of 550 °C with Ni/CaO–Al_2O_3 catalyst [30]. They did not only find low acetic acid conversion, but also that nickel catalyst, compared to noble metal catalyst (which is expensive), produced more coke formation on its surface [31]. Zhikun et al. mentioned that by increasing the Ni content in Ni/ZrO_2 catalyst up to 16%, the coke formation increased [32]. Besides, the Ni–CO supported on Lanthanum (III) Oxide was used inside the reformer to increase the reaction rate because Ni and noble based catalysts have been found to be more active and selective to hydrogen production and gave good hydrogen yields in acetic acid steam reformation [24]. On the other hand, cobalt-based catalyst is an appropriate catalyst for steam reforming of bio-oil due to its advantages of having no catalyst inventory cost and low temperature to generate high hydrogen yield. Besides, cobalt has the capability to promote C–C bond rupture at temperatures as low as 400 °C, and supported cobalt catalysts show higher production to H_2 and CO_2, but lower production to ethylene [33]. Furthermore, nickel and cobalt based catalysts required lower reaction temperature [34] and exhibited high activity and selectivity towards acetic acid conversion and hydrogen selectivity exceeded 90% [35]. Pudukudy et al. [6] were used Pd promoted Ni/SBA-15 for CH_4 decomposition. They found that Ni loading effect to block the catalyst pores and consequently decreased surface area of SBA-15. They mentioned that the Pd promoter increased the surface area and reduced the reduction temperature of NiO interacting with the SBA-15 due to the spillover effect of hydrogen. Other work done by Pudukudy et al. [36] regarding CH_4 decomposition over bimetallic Ni–Co/SBA-15 catalyst gives 56% of H_2 yield at 700 °C, but this catalyst found to have high coke formation. La_2O_3 had been chosen in this study as in the previous study, it showed good catalyst activity for acetic acid conversion and selectivity for hydrogen [37].

The purpose of this study was to appraise the reaction activity of bimetallic nickel (5 wt. %) and cobalt (5% wt.) supported on Lanthanum (III) oxide (90% wt.) on acetic acid steam reforming for hydrogen production. The study was carried out by varying the operating reaction temperature (500–800 °C) with the aim of getting the maximum catalytic activity and hydrogen production. The physical and the chemical properties of the catalyst catalysts were characterized by XRD, BET, H_2-TPR, TPD-NH_3 and CO_2, SEM, and TGA methods.

Experimental

Catalyst preparation

The impregnation method was used for preparing Ni–Co over La_2O_3. In order to prepare the catalyst, 10 wt. % of active metal (5 wt.% Ni and 5 wt.% Co) with 90 wt.% of La_2O_3 (all from Sigma–Aldrich). Ni–Co was obtained by aqueous solution of

Please cite this article in press as: Nabgan W, et al., Production of hydrogen via steam reforming of acetic acid over Ni and Co supported on La_2O_3 catalyst, International Journal of Hydrogen Energy (2016), http://dx.doi.org/10.1016/j.ijhydene.2016.04.176

cobalt nitrate hexahydrate (Co $(NO_3)_2 \cdot 6H_2O$) and Nickel nitrate hexahydrate (Ni $(NO_3)_2 \cdot 6H_2O$). Then, 9.00 g of La_2O_3 was mixed with 250 mL of heated de-ionized water, and later, the mixture was mixed with 4.94 g of (2.47 g Ni $(NO_3)_2 \cdot 6H_2O$/2.47 g Co $(NO_3)_2 \cdot 6H_2O$) catalyst based on Equation (1). In this equation, X is Ni $(NO_3)_2 \cdot 6H_2O$ or Co $(NO_3)_2 \cdot 6H_2O$. After that, the slurry was heated slowly to 90 °C while stirring at a maintained temperature (90 °C) until all the water had evaporated. Next, the solid residue was dried at 110 °C overnight in an oven. After that, the dried slurry was calcined at 750 °C for 3 h. Finally, the calcined slurry was crushed and filtered on two layers of 35 mesh (1.0 mm) and 34 mesh (1.4 mm) sieves.

$$Amount\ of\ X(g) = 0.5g\ Ni(or)Co \times \frac{1mol\ Ni(or)Co}{58.7g} \times \frac{1molX}{1mol\ Ni(or)Co} \times \frac{291g\ X}{1mol\ X} \quad (1)$$

Characterization of the samples

Powder XRD patterns were recorded with a Philips X-Pert 3710 diffractometer, by using a Cu Kα radiation at 40 kV and 30 mA. The 2θ angle was scanned with a rate of 1.5°/min within the range of $20° < 2\theta < 80°$. Besides, the BET method to the isotherms of N_2 adsorption was applied for catalyst specific surface area calculation, which had been calculated at the temperature of liquid nitrogen on a Beckman Coulter SA3100™ apparatus at 200 °C for 2 h on outgassed samples.

Meanwhile, the H_2 chemisorption at 25 °C by using a 30 mL/min flow rate of Ar and 0.1 mL (10% H_2 in Ar) on a Micromeritics Autochem II 2920 Chemisorption Analyser unit was used for Ni–Co dispersion measurement. The catalyst sample was reduced for 1 h at 650 °C under 30 mL/min H_2/Ar before the pulse chemisorption experiment was carried out. Then, the sample was flushed at 5 °C beyond the temperature reduction for 15 min under Ar gas.

Moreover, the same apparatus, Micromeritics Autochem II 2920 Chemisorption Analyzer, was used for temperature-programmed reduction (TPR) experiment, which was armed with a thermal conductivity detector. 25 mg of the catalyst was thermally treated to remove moisture, such water and other impurities, under 300 °C. Furthermore, in order to obtain the TPR profile, the sample was heated under 30 mL/min at 10% of H_2/Ar and a temperature range of 50–800 °C at the 15 °C/min linearly programmed rate.

In addition, thermogravimetric analysis (TGA) profiles were carried out in Perkin Elmer TGA instrument, which had been operated under nitrogen flowing at a heating rate of 10 °C/min. Besides, exothermic weight loss was observed at the temperature range between 30 and 950 °C. This could be assigned to the combustion of deposited carbon.

Activity test

The 0.36 mL/min acetic acid flow rate was fed into the reactor by employing a high pressure liquid chromatography (HPLC) pump (model: Pharmacia LKB 2850). After that, nitrogen was regulated at a flow rate of 30 mL/min, mixed with acetic acid solution, and then, it was pre-heated at 200 °C. The mixture, then, moved into a vapor phase and was fed into the fixed bed reactor at an atmosphere pressure. Besides, the temperature ranged from 500 °C to 700 °C, while the catalyst amount of 0.2 g was placed on a quartz reactor (12.7 mm O.D. and 10 mm I.D). The thermocouple was placed on the catalyst bed. The temperature of the reactor was controlled at the catalyst bed, and the temperature was measured by using a thermocouple (type-K). The flow diagram of this work is similar to that employed by Abdullah et al. [38].

Prior to the experiment, the catalyst was reduced in-situ with pure hydrogen at 30 mL/min and 600 °C for an hour. The reaction product obtained from the reactor flowed in a condenser, which was cooled by a circulating chiller set at 10 °C. Next, a liquid–gas separator was used to separate the liquid and the gas phases. The gas was examined through online gas chromatograph (model Agilent 6890N) armed with a thermal conductivity detector (TCD) and a capillary column (0.53 mm × 30 m CarboxenPlot. 1010). Other than that, the temperature of GC was 250 °C. Besides, 5 mL of liquid product was collected and stored in sample bottles. The samples of liquid were examined by using a Perkin Elmer GC armed with flame ignition detector (FID) and a capillary column (Nukol®).

Results and discussion

Catalyst characterizations

X-ray Diffraction

The X-ray diffraction (XRD) patterns of the various catalysts were shown in Fig. 1. The purpose of XRD is to investigate possible structural changes in the crystallinity of the catalysts after the reduction process at 600 °C. The characteristic diffraction peaks of metallic Ni° (111) [JCPDS 01-1258] and Co° (111) [JCPDS: 01-1254] are located at $2\theta = 44.4°$ [39] and were hard to distinguish from each other due to their similar morphology and characteristic peaks [40]. The absent of NiO or CoO signals could be explained by the fact that the

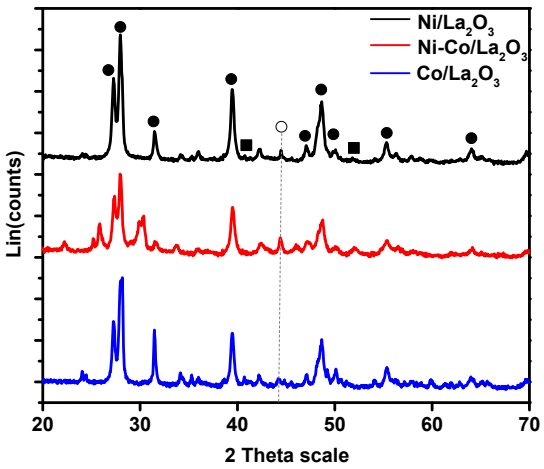

Fig. 1 – XRD patterns of Ni/La_2O_3, $Ni–Co/La_2O_3$ and Co/La_2O_3 catalysts (○) peaks correspond to Ni° and Co°, (●) peaks correspond to La_2O_3, (■) peaks correspond to $NiLaO_3$.

complete or partial reduction of NiO and CoO to metallic Ni° [41,42] and metallic Co° [43] is happened. The XRD patterns of La_2O_3 [JCPDS 02-0688 [44,45]] showed peaks at 2θ = 27.28, 27.93, 31.47, 39.52, 47.07, 48.63, 50.12, 55.36, and 64.04 representing the (1 1 1), (1 1 1), (2 0 0), (2 1 1), (2 2 0), (2 2 1), (2 2 1), (3 1 1), and (4 0 0) crystal plane of hexagonal phase respectively [45,46]. The additional peaks for the Ni/La_2O_3 and $Ni–Co/La_2O_3$ catalyst signals might be indexed to the $NiLaO_3$ phase which can be attributed to the strong interaction between Ni active metal and La_2O_3 support. Cubic perovskite-type of $NiLaO_3$ phase [JCPDS 33-0710 [47,48]] were observed for both Ni/La_2O_3 and $Ni–Co/La_2O_3$ catalysts at 2θ = 40.67 and 51.93 representing the (2 1 1) and (3 1 0) crystal plane, respectively.

Brunauer–Emmett–Teller (BET) surface area

The nitrogen adsorption isotherms of Ni and Co over La_2O_3 are shown in Fig. 2. After the active metals were added to the support, a large amount of micropores were generated and greatly enhanced the uptake of N_2 in low pressure regions. By adding cobalt in the catalyst, the N_2 adsorption increased significantly with the relative pressure in the whole pressure ranges. Moreover, the shape of the isotherms of the catalyst had been dependent on the active metals species introduced. The pore size distributions and N_2 adsorption/desorption isotherms of the reduced samples at different ranges of active metals showed that all the samples displayed mesoporous structure (Fig. 2b) while the quite large hysteresis loops in the isotherms indicated that the mesopores found in the Ni and Co over La_2O_3 are important (Fig. 2a). In addition, some parameters describing the porosity could be derived quantitatively from the adsorption data. Type IV isotherm, H_2 hysteresis loop, and typical mesoporous materials had been the categorizing aspects of nitrogen adsorption/desorption isotherms data, which means, solids consisted of particles crossed by nearly cylindrical channels or made by aggregates (consolidated) or agglomerates (unconsolidated) of spherical particles. Hence the addition of cobalt to Ni/La_2O_3 catalyst increased the mesoporous structure.

On top of that, the BET surface of catalyst exhibited different sizes of pores and an average pore diameter (see Table 1). Fig. 2b shows that for all of the catalyst samples, the pore size had been less than 20 nm with uniform distribution, while Co/La_2O_3 catalyst had the main pore size of about 10 nm. The high pore size and uniformity of Co/La_2O_3 catalyst benefited the uniform dispersion of metallic Ni/Co in the catalyst.

Support is needed in low surface areas and it is among the best known materials for physisorption of molecular hydrogen gas. Therefore, it had been important to determine the impacts of Ni and Co doping on the surface area of La_2O_3. The surface area calculated from nitrogen isotherm (Table 1) was found to be 15.06, 17.28, 7.79, and 0.6 m^2/g for Co/La_2O_3, $Ni–Co/La_2O_3$, Ni/La_2O_3, and bare La_2O_3 respectively, suggesting that Ni existed inside the pores and on the surface as well. It can be seen that the minimum particle size was 22.2 nm for Ni/La_2O_3 catalyst, but in general, the particle size was nearly in the same degree of instruction (22.2–25.6 nm).

Temperature-programmed reduction (TPR)

Fig. 3 illustrates the TPR-H_2 result profile for Ni–Co supported on La_2O_3 catalyst. These data show the dissimilar Ni–Co species relative properties to disperse the Ni–Co structure. The calcined catalyst shows the wide reduction peak in the range of 300–340 °C, 400 °C, and 550–700 °C, as portrayed in this figure. The first collection at about 400 °C temperatures could be attributed to the reduction of Ni and/or Co simple oxides, while the next peaks at over 600 °C temperatures could be ascribed to the reduction of spinel oxides. In fact, the presence of spinel phase could possibly stabilize the

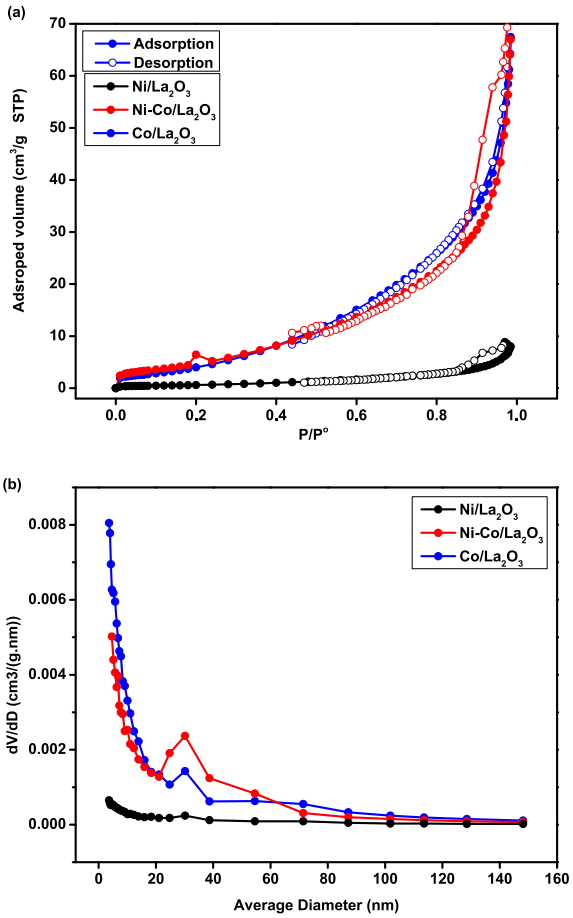

Fig. 2 – (a) N_2 adsorption and desorption isotherms and (b) pore size distribution of the as-prepared catalysts.

Table 1 – Chemical composition, BET surface area, pore volume, and average pore diameter of Ni/Co bimetallic catalysts.

	Ni (wt%)[a]	Co (wt%)[a]	S_{BET} (m^2/g)[b]	V_p (cm^3/g)[c]	D_p (nm)[d]
La_2O_3	0	0	0.6	0.004	22.1344
Ni/La_2O_3	9.88	0	7.79	0.0594	22.2323
$Ni–Co/La_2O_3$	4.96	4.99	17.28	0.0996	23.0556
Co/La_2O_3	0	9.99	15.06	0.0965	25.6274

[a] The metal content was measured by ICP test.
[b] S_{BET}, BET surface area.
[c] V_p, total pore volume.
[d] D_p, average pore diameter(4 V/S by BET).

Please cite this article in press as: Nabgan W, et al., Production of hydrogen via steam reforming of acetic acid over Ni and Co supported on La_2O_3 catalyst, International Journal of Hydrogen Energy (2016), http://dx.doi.org/10.1016/j.ijhydene.2016.04.176

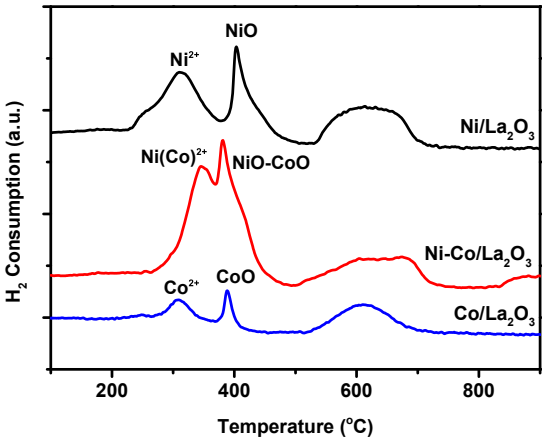

Fig. 3 – Ni–Co catalysts temperature-programmed reduction profiles of 10% vol H_2/Ar, and a heating rate at 10 °C/min.

formation of low size Ni metallic crystallites in reduction conditions, which exhibited a positive effect on conduct of reaction [49].

In addition, for all catalysts, the first peaks had been ascribable to the reduction of surface non-stoichiometric Ni(or Co)$^{3+}$ to Ni(or Co)$^{2+}$ [50], while the sharp peaks at 350–450 °C range catalyst had been due to the reduction of "unreacted" NiO (or CoO) on the surface, where this NiO form was essentially uninfluenced by the La support. On the other hand, as 50% and 0% of Ni catalysts samples showed a little, if any, hydrogen consumption, it could be concluded that the most reactive forms of NiO had undergone a progressive diffusion into the La_2O_3 lattice, likely forming a "bulk" Ni(or Co)O/La_2O_3 solid solution. Indeed, the reduction pattern of all samples (especially sample a) was characterized by a broad peak (600 °C), tailed towards higher temperature that denoted a reduction process evolving with a lower rate. This, together with the simultaneous decrease of NiO reducibility (see Table 2), had been the result of partial formation of "bulk" Ni(or Co)O/La_2O_3 solid solution. Moreover, it could be seen that the TPR peaks approved the dissimilar interaction degree for support species with metals that could eventually change the characterization of reduction. Nevertheless, the strong interaction of the active metal caused the reduction profile to shift to a higher temperature. Besides, the calculation of the area under the TPR curve (Table 2) showed that under the conditions applied, part of nickel was reduced (about 60%), which corresponded to the reduction of NiO only. These results confirmed XRD observations for reduced fresh catalyst where peaks of metallic Ni and La_2O_3 spinel phases were detected.

Table 2 – Relative total area of peaks.

Catalyst	CO_2 uptake (μmol/g)	H_2-consumption (μmol/g)	NH_3 uptake (μmol/g)
Ni/La_2O_3	153	1483	18,130
Ni–Co/La_2O_3	396	818	9719
Co/La_2O_3	132	259	12,960

Temperature-programmed desorption

The CO_2 TPD shapes on the catalysts displayed in Fig. 4a were executed after reduction process with pure hydrogen at 600 °C for an hour. In steam reforming of acetic acid, the active metal chemical nature plays an important part in the system catalytic performance; the active metal with strong basic characteristics, favors the facilitation of CO_2 adsorption (molecule with acid characteristics), and therefore, the gasification of the obtained carbonaceous deposits during the reaction, whereas those with strong acidity favor the growth of carbonaceous deposits [30]. Besides, the TPD-CO_2 profile shows the strong basic site at 473 °C, while weak sites at 555 °C and 727 °C for Ni/La_2O_3 catalyst, which has stronger basicity than 100 wt % of Co/La_2O_3, as shown in Table 2, based on peak area. Thus, the active metal becomes an "active oxygen" source species with high reactivity that leads to a path by which the coke deposition is prevented on the surface of catalyst. CO_2-TPD profiles from the Ni–Co/La_2O_3 catalyst were attained following CO_2 adsorption at 25 °C for 10 min. Moreover, it was practical for CO_2 to desorb from the Ni–Co/La_2O_3 catalyst, probably due to the amount of CO_2 desorbed was very low to be detected and/or because the CO_2 formed was powerfully adsorbed on the La_2O_3, e.g. in the form of La_2CO_3 that does not decompose in the functional range of temperature. In fact, a group of strong CO_2 peaks was detected to desorb from the Ni–Co/La_2O_3 catalyst.

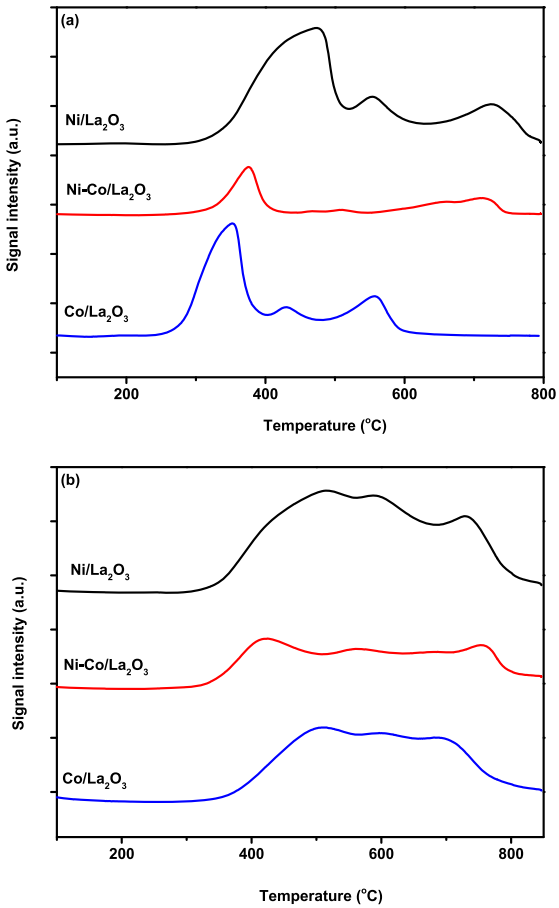

Fig. 4 – Temperature-programmed desorption of (a) CO_2 and (b) NH_3.

Please cite this article in press as: Nabgan W, et al., Production of hydrogen via steam reforming of acetic acid over Ni and Co supported on La_2O_3 catalyst, International Journal of Hydrogen Energy (2016), http://dx.doi.org/10.1016/j.ijhydene.2016.04.176

Furthermore, the acid properties of the catalysts varied with the type and the ratio of active metal. Fig. 4b shows the TPD-NH_3 profiles of La_2O_3 support-based catalysts and the data are presented in Table 2. The ammonia intensity deconvoluted curves were different for each catalyst. As for Ni/La and Co/La catalysts (a, b), a broad and strong NH_3 desorption peak at the temperature of 350~700 °C was observed, whereas weak desorption at 700~800 °C, and for Ni–Co/La catalyst, broad NH_3 desorption peaks with low intensity were observed within the temperature range of 350~800 °C. Besides, the area of NH_3 desorption peaks on Ni/La_2O_3 was larger than that of others, especially when it was mixed with cobalt (catalyst b), as shown in Table 2. That is to say, there were more acidic sites when nickel was doped into La_2O_3. Meanwhile for Co/La_2O_3, the area and the intensity of the desorption peaks of NH_3 decreased a little compared to that of Ni/La_2O_3 catalyst.

In addition, several aspects should be highlighted. For instance, bimetallic Ni–Co catalyst leads to the apparition of the weakest adsorption site of acid and the strongest base site, while the concentration of strong acid sites is higher than the concentration at strong base sites. Moreover, Ni-based catalyst has higher concentration of strong acid sites, but lower concentration at strong base sites. Besides, the deconvolution of the thermograms for the Ni/La_2O_3, Co/La_2O_3 and the Ni–Co/La_2O_3 catalysts evidenced two types of acid sites. Probably due to the basic character of La, this ratio of nickel and cobalt did not generate a new type of acid site. This may be a consequence of generating new acid sites specifically either to the interaction between the active metals and the support.

Catalysts performance tests

The catalytic performance of Ni/La_2O_3, Ni–Co/La_2O_3, and Co/La_2O_3 catalysts was examined under conditions of acetic acid steam reforming. The experiments were performed at temperature range of 500–700 °C using a 0.36 mL/min acetic acid flow rate and 0.2 g of catalyst. All catalysts were reduced with pure hydrogen at 30 mL/min and 600 °C for an hour. Fig. 5 compares the results collected in 6 h on stream, which shows differences in the total conversion and the product distribution depending on the catalysts used. It could be seen the catalyst showed activity for the reforming reactions even at the initial lower reaction temperature of 500 °C, where acetic acid conversion attained about 61.2%, 84.5%, and 91.5% for Co/La_2O_3, Ni–Co/La_2O_3, and Ni/La_2O_3 catalysts, respectively. The results of acetic acid conversion show that Co/La_2O_3 catalyst presents the poorest activity in acetic acid steam reforming reaction. This might be because of lowest hydrogen consumption on its surface which analyzed by H_2-

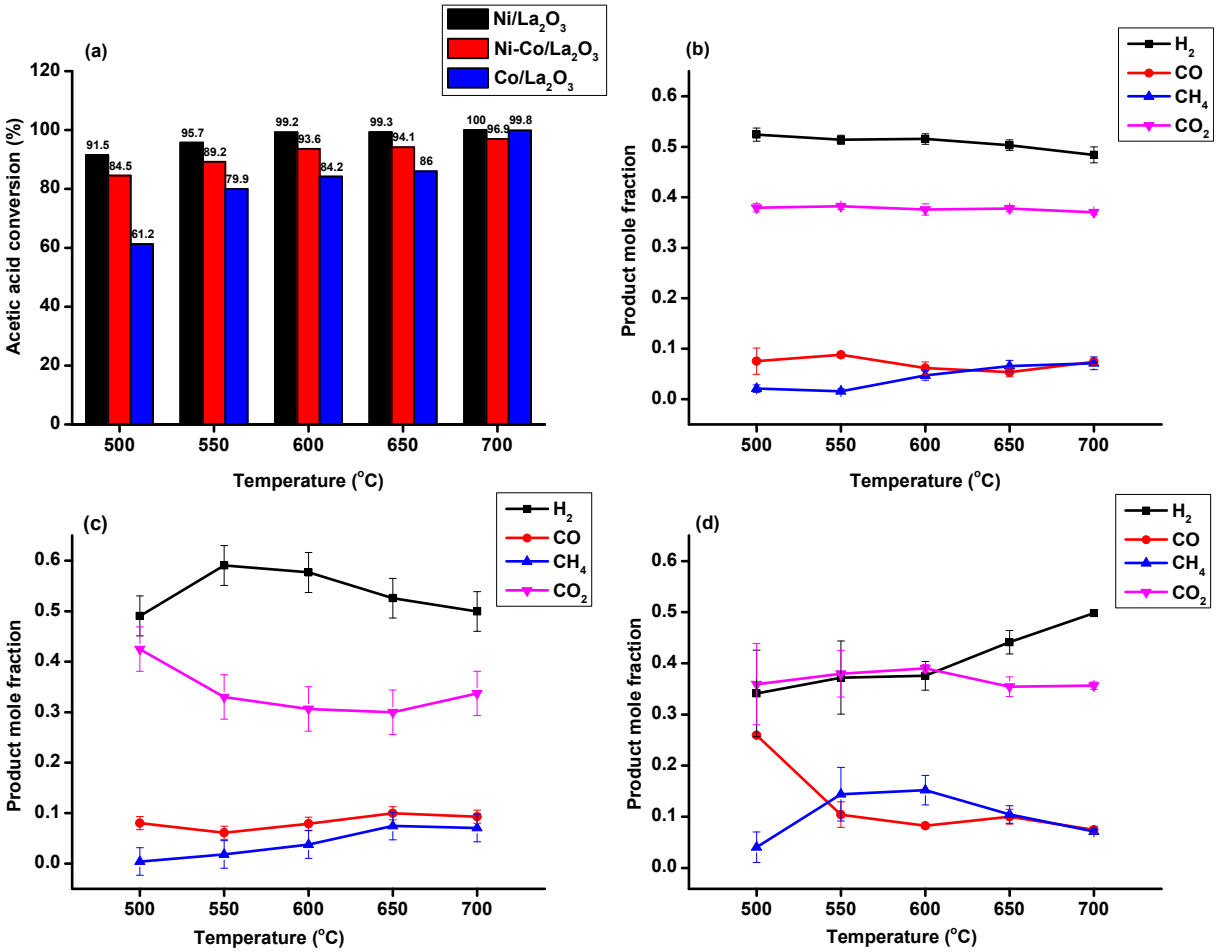

Fig. 5 – Effects of temperature on (a) acetic acid conversion; effect of temperature on product composition for (b) Ni/La_2O_3, (c) Ni-Co/La_2O_3, and (d) Co/La_2O_3 catalysts.

Please cite this article in press as: Nabgan W, et al., Production of hydrogen via steam reforming of acetic acid over Ni and Co supported on La_2O_3 catalyst, International Journal of Hydrogen Energy (2016), http://dx.doi.org/10.1016/j.ijhydene.2016.04.176

TPR. The most active catalyst is Ni/La_2O_3 with a conversion of 91.5% and an outlet H_2 molar fraction of 0.52 at 500 °C. The total conversion of acetic acid was achieved by increasing the temperature above 550 °C. Our result is consistent with results obtain for other catalysts [51–53] the highest activity of Ni/La_2O_3 catalyst towards acetic acid conversion might be due to highest hydrogen consumption, metal-support interaction and acidity behavior which analyzed by H_2-TPR and TPD-NH_3, respectively. This superior activity of Ni/La_2O_3 is in agreement with the work done by Zhikun et al. [54] who achieved complete conversion of acetic acid at 400 °C, S/C ratio 7.5:1; LHSV = 5.1 h^{-1}; P = 1 atm. According to previous literature [55,56], the catalytic activity was solely due to high Ni metal presented in the catalyst.

In addition, Fig. 5 shows the product mole fraction at reactor temperature ranged from 500 to 700 °C as well. There were four major products; H_2, CO, CH_4, and CO_2. As mentioned above, H_2 selectivity was observed to increase with increasing temperature, in accordance with thermodynamic predictions [57]. The general trend is similar to that observed for acetic acid conversion. At low temperatures, in decreasing order of H_2 selectivity, the result had been Ni/La_2O_3> $Ni–Co/La_2O_3$> Co/La_2O_3. This fact is in agreement with the preference of Ni^{2+} ions to occupy octahedral sites, as reported by other authors [58]. Moreover, with similar Ni and Co content catalysts, it can be seen that the mole fraction of H_2 increased until 550 °C, and then decreased. In contrast, CO_2 kept decreasing from 0.42 to 0.3, and after that, it decreased to 0.34 after 650 °C because of water gas shift reaction that favors high temperature. As predicted from the experimental result, due to competition of water gas shift reaction, H_2 dropped at 550 °C–700 °C, while the fractions of CH_4 and CO increased. The measured H_2 mole fraction at the high Ni catalyst resulted at about 0.2 higher than the mole fraction of high Co content catalyst for low temperature, while the rest exhibited similar values at high temperatures. Besides, Basagiannis et al. [27] mentioned that the reactions which may be taking place during steam reforming are water shift reaction, thermal decomposition, ketonization, and methanation, which are a combination of the exothermic and the endothermic reactions. As shown in Fig. 5 and Table 3, at high Ni catalyst, strong exothermic reactions had predominated.

The specialty of this work is that at 500–700 °C temperature range, the high conversion of acetic acid was achieved at 550 °C, which was 95.7% (Table 3), while the complete conversion was achieved at a temperature higher than 550 °C (see Fig. 5). Compared to other works, only lower temperature was needed for high acetic acid conversion and at high Ni catalyst, strong exothermic reactions had predominated. For example, Pant et al. [11] had used $Ni–Co/CeO_2/ZrO_2$ catalyst and 88% of acetic acid was converted to product due to the gradual oxidation of deposited carbon molecules.

Furthermore, the decomposition of carbon containing molecules had been produced into carbon oxides and hydrogen. A simple reaction mechanism for steam reforming of acetic acid is shown in Fig. 6, where it can be seen how acetic acid is proposed to decompose to CO_x and CH_x, whereas the latter species can react with OH-species; forming hydrogen and carbon oxides. Meanwhile, coke formation takes place either through oligomerization [59] or decomposition, as indicated in Fig. 6, which is the main problem related with this process as it causes relatively shorter lifetime of the catalyst [60,61].

Ni/La_2O_3 catalyst showed much better reforming activity compare to $Ni–Co/La_2O_3$ and Co/La_2O_3 catalysts, as the catalytic results presented above. Further we compare the performance of our Ni based catalyst with other Ni based catalyst on acetic acid steam reforming. There is however a few work studied the performance of Ni based catalyst on acetic acid steam reforming reaction. Basagiannis et al. [28] studied hydrogen production from acetic acid steam reforming using 17 wt.% $Ni/La_2O_3/Al_2O_3$ catalyst at H_2O/acetic acid molar ratio: 3, flow rate: 290 cm^3/min, T = 800 °C, P = 1 atm. They found that the acetic acid conversion fluctuated by time between 100% and 80% in a recurring periodic cycle. They found that the activity recovery under helium flow did not complete due to the coke deposition on the catalyst surface. On the other hand, Panagiotopoulou et al. [62] stated that the Ni based catalysts are active in the reforming reaction but prone to coke formation which leads to catalyst deactivation. Basagiannis et al. [27] also studied the acetic acid steam reforming using 17 wt.%$Ni/La_2O_3/Al_2O_3$ catalyst. They found the complete conversion of acetic acid to products at 950 °C but this catalyst prone to coke formation. However Xun et al. [35] found that Ni–Co bimetallic catalyst in acetic acid steam reforming reaction had good stability and resistance to carbon deposition at the experimental conditions of S/C mole ratio 7.5:1; LHSV = 5.1 h^{-1}; P = 1 atm compare to bare Ni metal and bare Co metal catalysts. The results obtained from previous research were comparable to our work. However, the catalyst preparation method, reaction condition, metal loading and promoter used is responsible for different activity and selectivity as well as the stability of the catalyst in the acetic acid steam reforming reaction.

Table 3 – Product distribution at 550 °C.

Catalyst	Acetic acid conversion	Products mole fraction			
		H_2	CO	CH_4	CO_2
Ni/La_2O_3	95.7	0.51	0.09	0.02	0.38
$Ni–Co/La_2O_3$	89.2	0.59	0.06	0.02	0.33
Co/La_2O_3	79.9	0.37	0.10	0.14	0.37

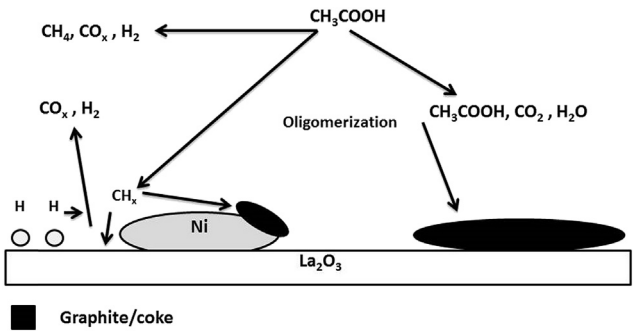

Fig. 6 – Functional reaction mechanism for the steam reforming of acetic acid.

Please cite this article in press as: Nabgan W, et al., Production of hydrogen via steam reforming of acetic acid over Ni and Co supported on La_2O_3 catalyst, International Journal of Hydrogen Energy (2016), http://dx.doi.org/10.1016/j.ijhydene.2016.04.176

TGA and SEM for spent catalysts

Thermogravimetric analysis (TGA) was carried out to determine the carbon deposition and heat evolved/absorbed during gravimetric loss up to 950 °C of all three spent catalysts, as shown in Fig. 7a. Besides, it had been identified that the TGA profiles showed different behaviors of weight loss. Moreover, Tsyganok et al. [63] explained the different behaviors of TGA profiles by temperature variation as follows. The initial weight reduction that appears in the TGA profile before temperatures reached 300 °C, as shown in Fig. 7a, is caused by the thermal desorption of H_2O and CO_2, as well as the removal of carbonaceous species that are easily oxidizable amorphous coke. The weight reduction at temperature higher than 500 °C is due to the gasification of whisker coke, where CO and CO_2 (CO_x) are generated through the oxidation of coke. In these spent catalysts, it is noted that the weight gain due to the oxidation of the metallic Ni particles on the surface is not observed between 400 and 450 °C. These results accord closely with a study carried out by Guo et al. concerning the TG data of used 5%Ni/$MgAl_2O_4$ spinel catalyst in CRM [64]. Besides, carbon deposition by Co contents shows that the least amount of coke (9.6%) was formed when Ni–Co/La_2O_3 was used, whereas the largest amount of coke (11.9%) was formed from the Ni/La_2O_3 catalyst without Co addition. The carbon deposition on the catalysts surface might be because of the coke deposition on the acid side of the catalyst and block the catalyst pores [65]. It is evident that the Co addition has a significant effect on the prevention of coke formation. Xun et al. [35] illustrated that the additional Co in Ni catalyst show the long term stability (70 h) in acetic acid steam reforming reaction. As mentioned above, amorphous carbonaceous species are oxidized at low temperature of 250–300 °C, while the oxidation of graphitic carbon occurs at high temperature over 500 °C. At the temperature where weight reduction occurs, the amount of amorphous carbon and graphitic carbon was estimated by dividing the sample weight for TGA analysis, respectively.

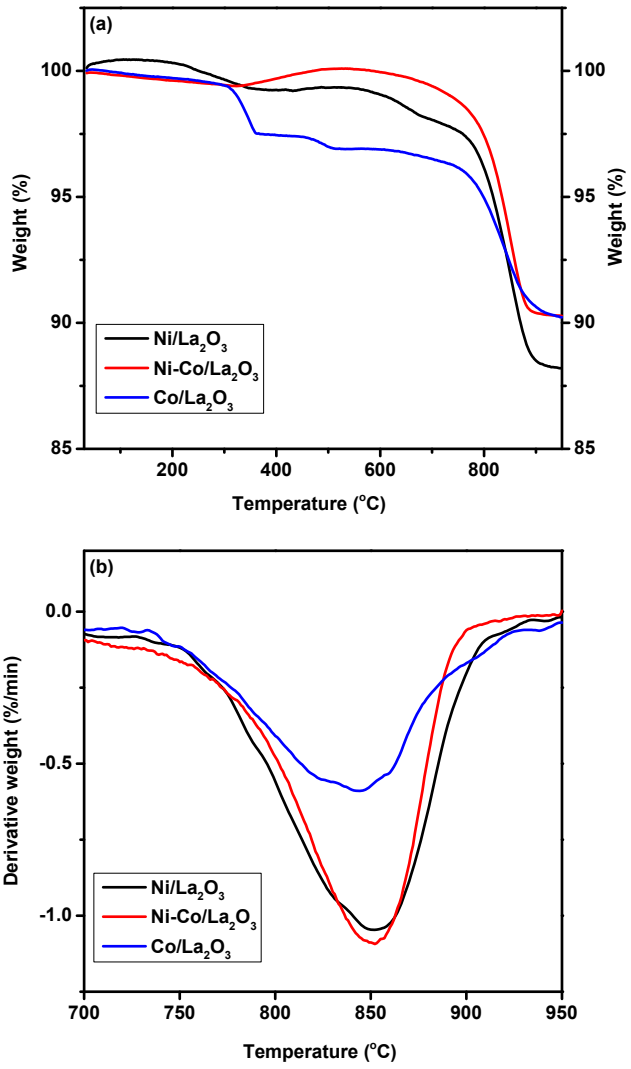

Fig. 7 – (a) TGA and (b) DTA curves after 6 h of steam reforming for Ni/La_2O_3, Ni–Co/La_2O_3, and Co/La_2O_3.

On top of that, the presence of three TG peak temperatures indicated that the same types of carbons were deposited on all catalysts pores (Fig. 7b). Nevertheless, the peak intensity of carbon T_{850} did not change as the nickel loading increased, but for higher nickel loading, more carbon was deposited in carbon T_{850}, as depicted from the TG-DTA. Besides, it had been reported that some acetate species that accumulated during the steam reforming remained stable up to about ±700 °C for all catalysts. In fact, the TG-DTA graph shown in Fig. 7b reveals that some of the species that accumulated on this catalyst might share a similar nature as acetate species that underwent decomposition with the help of O_2 at elevated temperatures. Other than that, the amount of coke formation was observed in all catalysts tested for 6 h.

The SEM images of Ni/Co over La_2O_3 calcined catalyst (fresh catalyst), after being experimented at 500 °C, 600 °C, and 700 °C, as shown in Fig. 8. In all samples, the observed particles with spherical morphology in any case of the composition were possible. The typical particle size of the Ni–Co/La_2O_3 before reduction sample was 2 μm, while for 500, 600, and 700 °C samples, the average particle size had been 1, 1.3, and 0.5 μm respectively. It can be seen that the surface carbon appeared to be denser on spent catalysts as compared to those that were fresh. This analysis of spent Ni–Co/La_2O_3 catalyst might suggest that the carbon formed was partially crystalline, with small crystallite sizes.

Conclusion

Steam reforming of acetic acid was investigated over Ni/La_2O_3, Ni–Co/La_2O_3, and Co/La_2O_3. Based on the catalysts characterization, the physicochemical description and the basicity measurement results presented the functionary of the catalyst that affected its reforming. The effect of surface enrichment of Co and the formation of Ni/Co alloy had been observed on the catalyst Ni–Co/La_2O_3. Besides, the synergetic effect between Ni and Co, the high dispersion of metals, and the uniform distribution of pore diameter caused an improvement in activity and anti-coking property of the catalyst. Nonetheless, adding Co into Ni/La_2O_3 decreased the coke formation and increased hydrogen selectivity. Besides, in

Please cite this article in press as: Nabgan W, et al., Production of hydrogen via steam reforming of acetic acid over Ni and Co supported on La_2O_3 catalyst, International Journal of Hydrogen Energy (2016), http://dx.doi.org/10.1016/j.ijhydene.2016.04.176

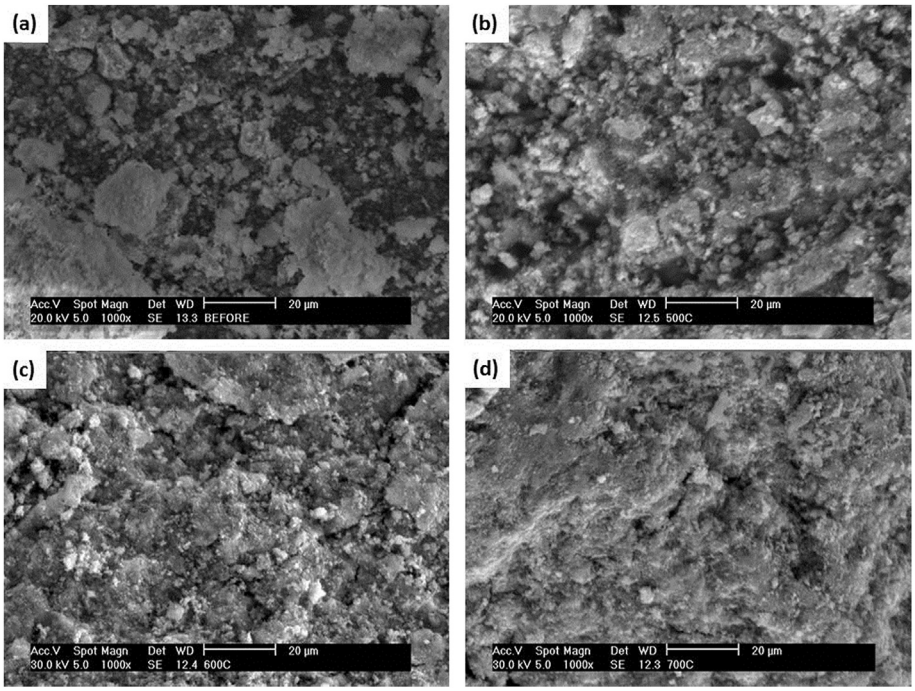

Fig. 8 – SEM micrographs of Ni–Co/La_2O_3 catalyst (a) fresh catalyst, (b) used catalyst at 500 °C steam reforming, (c) used catalyst at 600 °C steam reforming, (d) used catalyst at 700 °C steam reforming.

the experimental analysis of acetic acid steam reforming, H_2, CO, CH_4, and CO_2 were detected and the highest hydrogen produced was at temperature 550 °C. Thus, based on temperature effects on the catalyst, 550 °C offered the best performance in conversion of acetic acid with 95.7% for Ni/La_2O_3 catalyst with the highest ammonia desorption.

Acknowledgment

The authors acknowledge the financial support given for this work by Universiti Teknologi Malaysia under the Research University Grant (vot. 10H19) and Malaysia of Higher Education FRGS (vot. 4F478).

REFERENCES

[1] Huber GW, Iborra S, Corma A. Synthesis of transportation fuels from biomass: chemistry, catalysts, and engineering. Chem Rev 2006;106:4044–98.
[2] Mas V, Bergamini ML, Baronetti G, Amadeo N, Laborde M. A kinetic study of ethanol steam reforming using a nickel based catalyst. Top Catal 2008;51:39–48.
[3] Mariño F, Boveri M, Baronetti G, Laborde M. Hydrogen production from steam reforming of bioethanol using Cu/Ni/K/γ-Al2O3 catalysts. Effect of Ni. Int J Hydrogen Energy 2001;26:665–8.
[4] Cortright RD, Davda RR, Dumesic JA. Hydrogen from catalytic reforming of biomass-derived hydrocarbons in liquid water. Nature 2002;418:964–7.
[5] Verónica M, Graciela B, Norma A, Miguel L. Ethanol steam reforming using Ni(II)-Al(III) layered double hydroxide as catalyst precursor: kinetic study. Chem Eng J 2008;138:602–7.
[6] Pudukudy M, Yaakob Z, Akmal ZS. Direct decomposition of methane over Pd promoted Ni/SBA-15 catalysts. Appl Surf Sci 2015;353:127–36.
[7] Takanabe K, Aika K-i, Seshan K, Lefferts L. Sustainable hydrogen from bio-oil—Steam reforming of acetic acid as a model oxygenate. J Catal 2004;227:101–8.
[8] Bridgwater AV, Boocock DGB. Developments in thermochemical biomass conversion. Blackie Academic & Professional; 1997.
[9] Wang S, Zhang F, Cai Q, Li X, Zhu L, Wang Q, et al. Catalytic steam reforming of bio-oil model compounds for hydrogen production over coal ash supported Ni catalyst. Int J Hydrogen Energy 2014;39:2018–25.
[10] Takanabe K, K-i Aika, Seshan K, Lefferts L. Catalyst deactivation during steam reforming of acetic acid over Pt/ZrO2. Chem Eng J 2006;120:133–7.
[11] Pant KK, Mohanty P, Agarwal S, Dalai AK. Steam reforming of acetic acid for hydrogen production over bifunctional Ni–Co catalysts. Catal Today 2013;207:36–43.
[12] Wang C, Thygesen A, Liu Y, Li Q, Yang M, Dang D, et al. Bio-oil based biorefinery strategy for the production of succinic acid. Biotechnol Biofuels 2013;6:74.
[13] Zhao X, Davis K, Brown R, Jarboe L, Wen Z. Alkaline treatment for detoxification of acetic acid-rich pyrolytic bio-oil for microalgae fermentation: effects of alkaline species and the detoxification mechanisms. Biomass Bioenergy 2015;80:203–12.
[14] Stanbury PF, Whitaker A, Hall SJ. Principles of fermentation technology. Elsevier Science; 2013.
[15] Jarboe LR, Wen Z, Choi D, Brown RC. Hybrid thermochemical processing: fermentation of pyrolysis-derived bio-oil. Appl Microbiol Biotechnol 2011;91:1519–23.
[16] Zhao X, Chi Z, Rover M, Brown R, Jarboe L, Wen Z. Microalgae fermentation of acetic acid-rich pyrolytic bio-oil: reducing bio-oil toxicity by alkali treatment. Environ Prog Sustain Energy 2013;32:955–61.
[17] Vagia EC, Lemonidou AA. Thermodynamic analysis of hydrogen production via autothermal steam reforming of

selected components of aqueous bio-oil fraction. Int J Hydrogen Energy 2008;33:2489–500.
[18] Vagia EC, Lemonidou AA. Thermodynamic analysis of hydrogen production via steam reforming of selected components of aqueous bio-oil fraction. Int J Hydrogen Energy 2007;32:212–23.
[19] Garcia La, French R, Czernik S, Chornet E. Catalytic steam reforming of bio-oils for the production of hydrogen: effects of catalyst composition. Appl Catal A General 2000;201:225–39.
[20] Assaf PGM, Nogueira FGE, Assaf EM. Ni and Co catalysts supported on alumina applied to steam reforming of acetic acid: representative compound for the aqueous phase of bio-oil derived from biomass. Catal Today 2013;213:2–8.
[21] Cheng F, Dupont V. Nickel catalyst auto-reduction during steam reforming of bio-oil model compound acetic acid. Int J Hydrogen Energy 2013;38:15160–72.
[22] Wang D, Montané D, Chornet E. Catalytic steam reforming of biomass-derived oxygenates: acetic acid and hydroxyacetaldehyde. Appl Catal A General 1996;143:245–70.
[23] Lan P, Lan LH, Xie T, Liao AP. The preparation of syngas by the reforming of bio-oil in a fluidized-bed reactor. Energy Sources, Part A Recovery, Util Environ Eff 2014;36:242–9.
[24] Galvita VV, Semin GL, Belyaev VD, Semikolenov VA, Tsiakaras P, Sobyanin VA. Synthesis gas production by steam reforming of ethanol. Appl Catal A General 2001;220:123–7.
[25] Wilhelm DJ, Simbeck DR, Karp AD, Dickenson RL. Syngas production for gas-to-liquids applications: technologies, issues and outlook. Fuel Process Technol 2001;71:139–48.
[26] Fatsikostas AN, Kondarides DI, Verykios XE. Production of hydrogen for fuel cells by reformation of biomass-derived ethanol. Catal Today 2002;75:145–55.
[27] Basagiannis AC, Verykios XE. Reforming reactions of acetic acid on nickel catalysts over a wide temperature range. Appl Catal A General 2006;308:182–93.
[28] Basagiannis AC, Verykios XE. Catalytic steam reforming of acetic acid for hydrogen production. Int J Hydrogen Energy 2007;32:3343–55.
[29] Hu X, Lu G. Investigation of the steam reforming of a series of model compounds derived from bio-oil for hydrogen production. Appl Catal B Environ 2009;88:376–85.
[30] Vagia EC, Lemonidou AA. Hydrogen production via steam reforming of bio-oil components over calcium aluminate supported nickel and noble metal catalysts. Appl Catal A General 2008;351:111–21.
[31] Hu X, Dong D, Zhang L, Lu G. Steam reforming of bio-oil derived small organics over the Ni/Al2O3 catalyst prepared by an impregnation–reduction method. Catal Commun 2014;55:74–7.
[32] Li Z, Hu X, Zhang L, Liu S, Lu G. Steam reforming of acetic acid over Ni/ZrO2 catalysts: effects of nickel loading and particle size on product distribution and coke formation. Appl Catal A General 2012;417–418:281–9.
[33] Llorca J, Homs Ns, Sales J, de la Piscina PRr. Efficient production of hydrogen over supported cobalt catalysts from ethanol steam reforming. J Catal 2002;209:306–17.
[34] Pudukudy M, Yaakob Z, Takriff MS. Methane decomposition over Pd promoted Ni/MgAl2O4 catalysts for the production of COx free hydrogen and multiwalled carbon nanotubes. Appl Surf Sci 2015;356:1320–6.
[35] Hu X, Lu G. Investigation of steam reforming of acetic acid to hydrogen over Ni–Co metal catalyst. J Mol Catal A Chem 2007;261:43–8.
[36] Pudukudy M, Yaakob Z, Akmal ZS. Direct decomposition of methane over SBA-15 supported Ni, Co and Fe based bimetallic catalysts. Appl Surf Sci 2015;330:418–30.
[37] Dantas SC, Escritori JC, Soares RR, Hori CE. Effect of different promoters on Ni/CeZrO2 catalyst for autothermal reforming and partial oxidation of methane. Chem Eng J 2010;156:380–7.
[38] Abdullah TAT, Nabgan W, Kamaruddin MJ, Mat R, Johari A, Ahmad A. Hydrogen production from acetic acid steam reforming over bimetallic Ni-Co on La2O3 catalyst- Effect of the catalyst dilution. Appl Mech Mater 2014;493:39–44.
[39] Zhao L, Han T, Wang H, Zhang L, Liu Y. Ni-Co alloy catalyst from LaNi1–xCoxO3 perovskite supported on zirconia for steam reforming of ethanol. Appl Catal B Environ.
[40] Xu J, Zhou W, Li Z, Wang J, Ma J. Biogas reforming for hydrogen production over nickel and cobalt bimetallic catalysts. Int J Hydrogen Energy 2009;34:6646–54.
[41] Cabo M, Garroni S, Pellicer E, Milanese C, Girella A, Marini A, et al. Hydrogen sorption performance of MgH2 doped with mesoporous nickel- and cobalt-based oxides. Int J Hydrogen Energy 2011;36:5400–10.
[42] Han SJ, Bang Y, Yoo J, Seo JG, Song IK. Hydrogen production by steam reforming of ethanol over mesoporous Ni–Al2O3–ZrO2 xerogel catalysts: effect of nickel content. Int J Hydrogen Energy 2013;38:8285–92.
[43] Lin SSY, Kim DH, Ha SY. Metallic phases of cobalt-based catalysts in ethanol steam reforming: the effect of cerium oxide. Appl Catal A General 2009;355:69–77.
[44] Zhang G, Zhang S, Yang L, Zou Z, Zeng D, Xie C. La2O3-sensitized SnO2 nanocrystalline porous film gas sensors and sensing mechanism toward formaldehyde. Sens Actuators B Chem 2013;188:137–46.
[45] Fleming P, Farrell RA, Holmes JD, Morris MA. The rapid formation of La(OH)3 from La2O3 powders on exposureto water vapor. J Am Ceram Soc 2010;93:1187–94.
[46] Sutthiumporn K, Kawi S. Promotional effect of alkaline earth over Ni–La2O3 catalyst for CO2 reforming of CH4: role of surface oxygen species on H2 production and carbon suppression. Int J Hydrogen Energy 2011;36:14435–46.
[47] Yang Z, Huang Y, Dong B, Li H-L. Template induced sol–gel synthesis of highly ordered LaNiO3 nanowires. J Solid State Chem 2005;178:1157–64.
[48] Yang X, Li S, Liu Y, Wei X, Liu Y. LaNi0.8Co0.2O3 as a cathode catalyst for a direct borohydride fuel cell. J Power Sources 2011;196:4992–5.
[49] Benito M, García S, Ferreira-Aparicio P, Serrano LG, Daza L. Development of biogas reforming Ni-La-Al catalysts for fuel cells. J Power Sources 2007;169:177–83.
[50] Highfield JG, Bossi A, Stone FS. Dispersed-Metal/Oxide catalysts prepared by reduction of high surface area oxide solid solutions. In: Poncelet G, Grange P, Jacobs PA, editors. Studies in surface science and catalysis. Elsevier; 1983. p. 181–92.
[51] Wang Q, Wang S, Li X, Guo L. Hydrogen production via acetic acid steam reforming over HZSM-5 and Pd/HZSM-5 catalysts and subsequent mechanism studies. 2013.
[52] Hu X, Lu G. Acetic acid steam reforming to hydrogen over Co–Ce/Al2O3 and Co–La/Al2O3 catalysts—The promotion effect of Ce and La addition. Catal Commun 2010;12:50–3.
[53] Vagia EC, Lemonidou AA. Investigations on the properties of ceria–zirconia-supported Ni and Rh catalysts and their performance in acetic acid steam reforming. J Catal 2010;269:388–96.
[54] Li Z, Hu X, Zhang L, Lu G. Renewable hydrogen production by a mild-temperature steam reforming of the model compound acetic acid derived from bio-oil. J Mol Catal A Chem 2012;355:123–33.
[55] Thaicharoensutcharittham S, Meeyoo V, Kitiyanan B, Rangsunvigit P, Rirksomboon T. Hydrogen production by steam reforming of acetic acid over Ni-based catalysts. Catal Today 2011;164:257–61.

Please cite this article in press as: Nabgan W, et al., Production of hydrogen via steam reforming of acetic acid over Ni and Co supported on La_2O_3 catalyst, International Journal of Hydrogen Energy (2016), http://dx.doi.org/10.1016/j.ijhydene.2016.04.176

[56] Hu X, Zhang L, Lu G. Pruning of the surface species on Ni/Al2O3 catalyst to selective production of hydrogen via acetone and acetic acid steam reforming. Appl Catal A General 2012;427–428:49–57.
[57] Koh ACW, Chen L, Kee Leong W, Johnson BFG, Khimyak T, Lin J. Hydrogen or synthesis gas production via the partial oxidation of methane over supported nickel–cobalt catalysts. Int J Hydrogen Energy 2007;32:725–30.
[58] Hierl R, Knözinger H, Urbach H-P. Surface properties and reduction behavior of calcined CuOAl2O3 and CuO-NiOAl2O3 catalysts. J Catal 1981;69:475–86.
[59] Zhang Q, Chang J, Wang T, Xu Y. Review of biomass pyrolysis oil properties and upgrading research. Energy Convers Manag 2007;48:87–92.
[60] Rioche C, Kulkarni S, Meunier FC, Breen JP, Burch R. Steam reforming of model compounds and fast pyrolysis bio-oil on supported noble metal catalysts. Appl Catal B Environ 2005;61:130–9.
[61] Bazin D, Borkó L, Koppány Z, Kovács I, Stefler G, Sajó LI, et al. Re-Co/NaY and Re-Co/Al2O3 bimetallic catalysts: in situ EXAFS study and catalytic activity. Catal Lett 2002;84:169–82.
[62] Panagiotopoulou P, Papadopoulou C, Matralis H, Verykios X. Production of renewable hydrogen by reformation of biofuels. Wiley Interdiscip Rev Energy Environ 2014;3:231–53.
[63] Tsyganok AI, Tsunoda T, Hamakawa S, Suzuki K, Takehira K, Hayakawa T. Dry reforming of methane over catalysts derived from nickel-containing Mg–Al layered double hydroxides. J Catal 2003;213:191–203.
[64] Guo J, Lou H, Zhao H, Chai D, Zheng X. Dry reforming of methane over nickel catalysts supported on magnesium aluminate spinels. Appl Catal A General 2004;273:75–82.
[65] Hoffmann J. Bio-oil production-process optimization and product quality: Videnbasen for Aalborg UniversitetVBN. 2013. Aalborg UniversitetAalborg University, Det Teknisk-Naturvidenskabelige FakultetThe Faculty of Engineering and Science.

Please cite this article in press as: Nabgan W, et al., Production of hydrogen via steam reforming of acetic acid over Ni and Co supported on La_2O_3 catalyst, International Journal of Hydrogen Energy (2016), http://dx.doi.org/10.1016/j.ijhydene.2016.04.176